Geometries for Streamflow Measurement Using a UHF RiverSonde

Calvin C. Teague, Donald E. Barrick, and Peter M. Lilleboe
CODAR Ocean Sensors, Ltd.
Los Altos, California 94024
(408) 773-8240, fax (408) 773-0514
cal@alpha.stanford.edu, COSDon@aol.com, pete@codaros.com

***Abstract*— Three geometries for a UHF streamflow radar system are examined: bistatic across the channel, monostatic on a bank, and monostatic in the center of the channel. The radar operates by analyzing the frequency spectrum of the received energy and determining the angles of arrival of energy at each frequency, so it is important to understand how the various geometries affect the width of the frequency spectrum and its angular distribution. We argue that placing the radar and antenna on one bank, with the antennas looking broadly across the river, generally produces the best results. The broad frequency spectrum allows many points to be analyzed, most of which have single-angle direction solutions (which generally are more robust than dual-angle solutions), and all the equipment can be placed at a single location.**

I. Introduction

Three different geometries for a RiverSonde UHF streamflow radar system have been used in field experiments. The first experiments were done using a bistatic configuration, with the transmitting antenna on one side of a river or canal and the receiving antenna on the other side [1]. Subsequent experiments made use of a monostatic geometry, with the transmitter and receiver on one bank of a river and the field of view broadly across the river, looking both upstream and downstream [2]. Another monostatic configuration placed the transmitter and receiver on a bridge spanning a canal with the antennas looking narrowly upstream. The three configurations are sketched in Fig. 1. Each configuration has its advantages and disadvantages.

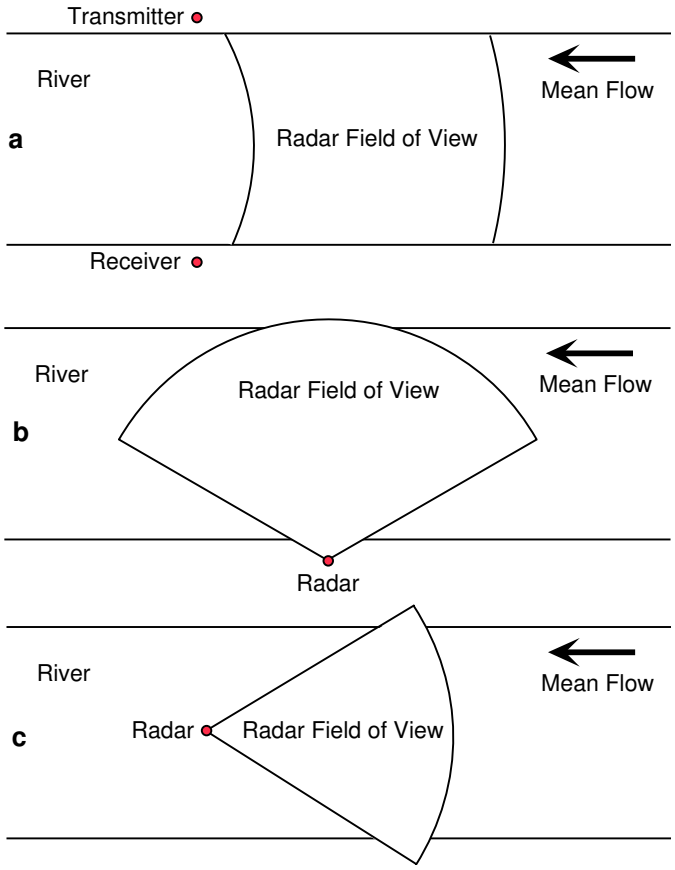

Fig. 1. Three RiverSonde geometries. (a) Bistatic with the transmitter on one bank and the receiver on the opposite bank, looking upstream or downstream. (b) Monostatic with radar on a bank, looking broadly across the channel in both upstream and downstream directions. (c) Monostatic with radar in the center of the channel, looking upstream or downstream.

II. Model

A comprehensive analysis of the three geometries is beyond the scope of this article, so their performance based on a simple model will be considered. A radar center frequency of 335 MHz is assumed, with a radar wavelength of 0.90 m and a Bragg-resonant water wavelength of 0.45 m at grazing incidence. The RiverSonde radar works by Fourier processing of the received energy to determine its Doppler shift (and hence radial velocity), and then determining the direction(s) of the signals, at each frequency bin, producing that Doppler shift. The RiverSonde uses MUSIC direction finding [3] with 3 antennas, so it is possible to resolve up to 2 directions of arrival for each frequency bin. The system works best when the received signals are spread over a broad frequency range, and signals from no more than 2 directions (preferably just one direction) arrive at each frequency.

For the river model, assume a straight water channel of width $2W = 70$ m with a flow which varies only in the cross-channel direction as shown in Fig. 2. The assumed flow varies across the channel as $c_m(0.6 + 0.4\cos\pi y/2W)$ with y ranging from $-W$ to $+W$. Two cases are considered, with the maximum flow $c_m = 1.0$ or 2.5 m/s. The radar antennas are assumed to be on the banks 15 m from the edge of the

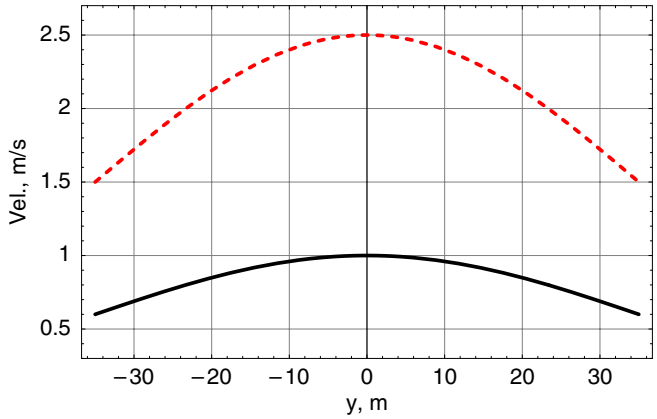

Fig. 2. Assumed flow variation as a function of cross-channel distance y. Two profiles with maximum velocities of 1.0 and 2.5 m/s are analyzed.

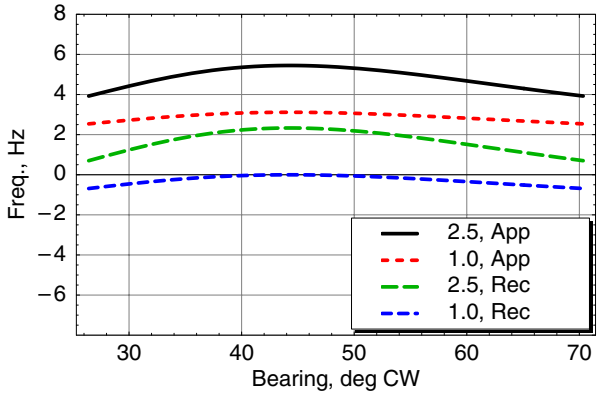

Fig. 3. Bistatic: Doppler shift as a function of bearing at the receiver, measured positive clockwise from the transmit antenna, assumed directly opposite the receive antenna. Data for maximum flow rates of 1.0 and 2.5 cm/s are shown, for energy scattered by waves approaching or receding from the radar.

water, or in the center of the channel (perhaps mounted on a bridge), all at a height of 5 m above the surface of the water. The performance of each geometry is analyzed in terms of the Doppler shift of the received signals from a slant range of 50 m, or in the case of the bistatic geometry, approximately 50 m upstream of the antennas, as a function of bearing angle at the receiver measured clockwise from the nominal receive antenna broadside look direction.

III. Bistatic

The bistatic geometry of Fig. 1a was chosen for the first experiments [1] because it has the advantage that the scattered signal strength is relatively constant across the width of the channel, since the total path length from transmitter to scattering patch to receiver remains relatively constant for various positions of the scattering patch across the channel. However, data interpretation is complicated because lines of constant delay are ellipses rather than circles, the wavelength of the Bragg-resonant water waves (which determines their phase velocity) is not just half the radio wavelength but depends

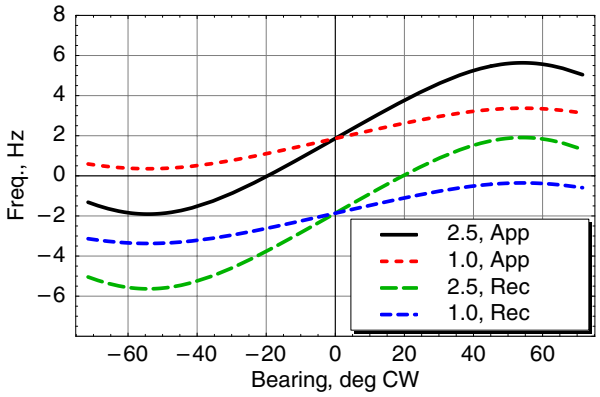

Fig. 4. Monostatic on bank: Doppler shift as a function of bearing at the receiver, measured positive clockwise from a direction perpendicular to the bank. Data for maximum flow rates of 1.0 and 2.5 cm/s are shown, for energy scattered by waves approaching or receding from the radar.

on the scattering angle, and the direction of the Bragg waves is not along the radar radial direction but bisects the scattering angle; all of these effects vary with position on the water [4].

Fig. 3 shows the received Doppler frequency as a function of bearing for a total path length of 40 m greater than the 100 m distance from transmit to receive antennas, which corresponds to a scattering region 42–49 m upstream of the antennas. In general, energy is received from waves both approaching and receding from the radar, and curves are shown for two different maximum flow values. The Doppler shift for the bistatic case is complicated by the fact that the Doppler shift due to the waves alone is a minimum in the center of the channel, while the Doppler shift due to the flow usually is a maximum in the center of the channel for realistic flow profiles. In certain cases, the sum of these two components can result in in almost no variation of total Doppler shift as a function of angle. In this case, the Doppler shift extends over about 0.75 Hz for a maximum flow of 1.0 m/s. The Bragg-resonant wavelength and projected velocity vector in the direction of the bistatic antennas depends on the scattering angle between vectors from the scattering patch to the two antennas, and this angle depends on distance along the river, with the angle becoming zero in the limiting case of very long ranges.

IV. Monostatic on Bank

Although the monostatic geometries result in more signal strength variation with range than the bistatic geometry, the wavelength of the Bragg waves is simply half the radio wavelength (unless there is a significant depression angle to the water), and the propagation direction of the Bragg-resonant waves is along the radar radial direction. In practice the range-dependent signal strength variation has not been a serious limitation. With the radar on one bank as in Fig. 1b, the Doppler shift due to the channel flow viewed over a broad range of angles (up to 140° in some cases) results in a very broad frequency spectrum illustrated in Fig. 4, with the energy in most frequency bins coming from a single direction for low

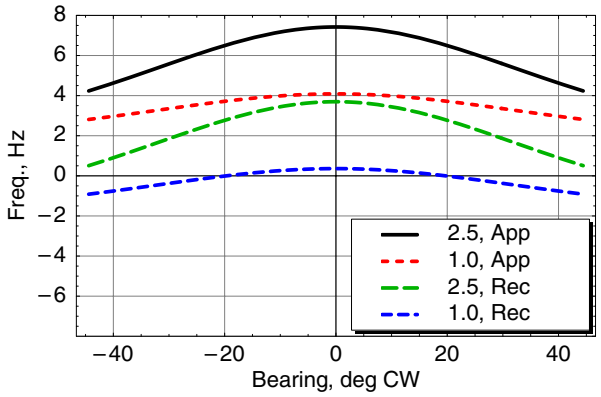

Fig. 5. Monostatic at center: Doppler shift as a function of bearing at the receiver, measured positive clockwise from a direction parallel to the bank. Data for maximum flow rates of 1.0 and 2.5 cm/s are shown, for energy scattered by waves approaching or receding from the radar.

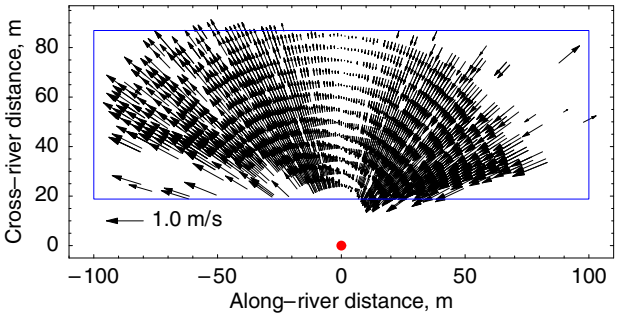

Fig. 6. Radial water flow for one 2.5-minute data segment on May 8, 2002 at Vernalis, California on the San Joaquin River. Spurious vectors caused by personnel movement near the antennas have been removed using a median filter but otherwise the vectors indicate the raw data. Approximately 2500 radial vectors are plotted. The radar location is indicated by the dot at the origin.

flow velocities. For a maximum flow of 1.0 m/s, the width of the frequency spectrum is about 3.0 Hz. However, at higher velocities, as in the example of 2.5 m/s, it is possible for energy from both approaching and receding waves to appear at the same Doppler frequency, as shown in Fig. 4. Furthermore, if the flow velocity drops significantly near the banks, there can be small frequency regions where there are dual-angle returns even for low flow velocity. Note that this study does not address the relative amplitudes of these signals, so in practice the multiple-angle returns may not be a serious problem.

V. Monostatic in Center

The radar can also be placed on a bridge or other support in the middle of the water channel as shown in Fig. 1c. Generally this results in a much narrower frequency spectrum, illustrated in Fig. 5, than obtained from the bank, with fewer frequency bins to cover the observed flow distribution. For a maximum flow rate of 1.0 m/s, the width of the spectrum is about 1.5 Hz. However, the narrower width actually may be advantageous in the case of high flow rates, because the energy from the approaching and receding waves is less likely to overlap (compare Figs. 4 and 5 for the 2.5 m/s flow rate). For high flow rates, dual-angle solutions are possible even for the radar on a bank, and the separation of the energy from approaching and receding waves may be better defined with the radar in the center than on a bank.

VI. Discussion

Although the bistatic geometry has the apparent advantage of less variation in signal strength as a function of location of the scattering patch, it appears to have a disadvantage in terms of spreading the received energy in frequency. It also requires either a cable across the channel for the transmit or receive antennas or two separate radar units, one on either side of the channel, which must be synchronized together and separately powered. The monostatic geometries, on the other hand, spread the frequency of the scattered energy over a wider range and concentrate the equipment in a single location. The geometry of Fig. 1b with the radar on a bank appears to be preferable for low flow velocities on the order of the phase velocity of the Bragg waves or less, because most of the energy comes from a single direction at a given frequency and the frequency spectrum is broad. For higher flow velocities, where the bank configuration results in dual-angle returns from approaching and receding Bragg energy, the configuration of Fig. 1c with the radar in the center of the channel may be attractive.

An example of data obtained from a river bank is shown in Fig. 6. This figure displays radial flow vectors obtained from a 2.5-minute segment of data recorded at Vernalis, California on the bank of the San Joaquin river [2]. The river was approximately 70 m wide at the radar site, and the flow rate was on the order of 1.0 m/s in the middle of the channel, dropping to about 0.6 m/s near the banks, although somewhat more abruptly than the model of Fig. 2. The RiverSonde UHF radar was operated at a center frequency of 335 MHz with a range resolution of 5 m and a velocity resolution of 2.5 cm/s. Water flow rates measured from the radar, at an effective depth of about 4 cm, generally agree to within about 10 cm/s with *in-situ* flow measurements at a depth of about 11 cm, with the radar measurements about 10% higher than the *in-situ* measurements [2].

References

[1] Calvin C. Teague, Donald E. Barrick, Peter Lilleboe, and Ralph T. Cheng, "Canal and river tests of a RiverSonde streamflow measurement system," in *IEEE 2001 International Geoscience and Remote Sensing Symposium Proceedings*, New York, July 2001, IEEE, pp. 1288–1290, IGARSS'01, Sydney, Australia.

[2] Calvin C. Teague, Donald E. Barrick, Peter M. Lilleboe, and Ralph T. Cheng, "Initial river test of a monostatic riversonde streamflow measurement system," in *Proc. of the IEEE/OES Seventh Working Conference on Current Measurement Technology*, Judith A. Rizoli, Ed., New York, March 2003, IEEE, pp. 46–50.

[3] R. O. Schmidt, "Multiple emitter location and signal parameter estimation," *IEEE Trans. on Antennas and Propagation*, vol. AP-34, pp. 276–280, 1986.

[4] C. C. Teague, "Bistatic radar techniques for observing long wavelength directional ocean-wave spectra," *IEEE Trans., Geoscience Electronics*, vol. GE-9, no. 4, pp. 211–215, Oct 1971.